Iran University of Science and Technology

Automotive Science and Engineering

Journal Homepage: ase.iust.ac.ir

ISSN: 2008-9899

Lateral Motion Control of In-Wheel Motor EVs via Optimal Energy-Efficient Control Allocation

Milad Sarani[1], Behrooz Mashadi[1], Majid Majidi[2*]

[1] School of Automotive Engineering, Iran University of Science and Technology, Tehran, Iran.

[2] Department of Mechanical Engineering, Qa.C., Islamic Azad University, Qazvin, Iran.

E-mail: majid.majidi@iau.ac.ir

ARTICLE

Article history:
Received : 18 Jun 2025
Accepted: 27 Dec 2025
Published: 30 Jan 2026

Control allocation
EV
Sliding mode control
Stability control
optimization

A B S T R A C T

In this paper, a multi-level hierarchical control method for enhancing electric vehicle (EV) stability with four independent in-wheel motors is proposed. In the high-level motion controller, a sliding mode controller is used to calculate the total desired force and yaw moment, and in the low-level control allocation, an optimal energy-efficient control allocation scheme is presented to provide optimally distributed torques for four in-wheel motors. Moreover, both handling performance and energy savings are investigated in this research and evaluated via a co-simulation approach using MATLAB/Simulink, and CarSim. With a torque distribution algorithm based on energy efficiency optimization, the EV is controlled with and without a controller in J-turn and lane change maneuvers. The simulation results show that the proposed torque control system and torque distribution algorithm can maintain stability, reduce energy consumption, and track the desired values of yaw rate and longitudinal velocity of the vehicle in the mentioned maneuvers

1. Introduction

As far as environmental pollution is concerned, electric vehicles (EVs) which are also known as zero-emission vehicles play a central role in transportation systems all over the world. With the current bottleneck in the increase of battery energy density, effective driving energy management has become critical for enhancing the driving range of electric vehicles and achieving energy conservation. The development of advanced drive technologies for EVs may lead to the implementation of high-efficiency driving energy management strategies, which could further enhance their driving range [1]. A novel layout used for EVs is to exploit electric motors in the inner space of each wheel. In EVs equipped with in-wheel motors, a wheel torque controller allows for the independent allocation of driving and braking torques among the vehicle wheels. The highlighted advantage of in-wheel motors EVs is accompanied by a strong emphasis on stability management for these vehicles. As a result, recent research endeavors primarily strive to enhance the lateral stability of EVs during critical maneuvers.

When it comes to vehicle lateral dynamics control, the yaw rate is the primary control variable. Moreover, the sideslip angle of the

*Corresponding Author
Email: majid.majidi@iau.ac.ir
http://doi.org/10.22068/ase.2026.725

[DOI: 10.22068/ase.2026.725]

vehicle is another control variable kept limited by controlling the vehicle angular velocity of the vehicle in this paper. Thus, a corrective yaw moment generated by the direct yaw moment control (DYC) system is designed to track the desired vehicle yaw rate which in turn keeps the vehicle sideslip angle restricted. In general, DYC systems are categorized into two main systems which are differential braking system (DBS) and torque vectoring (TV) system which use asymmetric braking and driving longitudinal forces respectively to create the corrective yaw moment required to ensure that the vehicle's states remain at the desired values. From the point that the driving and braking torques of in-wheel-motor EVs can be controlled independently for each wheel, this type of electric powertrain is the best choice for designing a DYC system. Therefore, electric vehicles have been the focus of interest among researchers in recent years [2].

Mashadi and Majidi [3] proposed the idea of using two electric motors embedded in the rear wheels to apply the direct yaw moment to improve the vehicle stability at different maneuvers. The idea has advantages over conventional ESC systems including solving the braking problem, which affects the vehicle longitudinal dynamics.

In reference [4], a control algorithm is proposed for optimizing driving efficiency, satisfying driver demands, and considering tire slip and vehicle cornering. Besides, a fuzzy controller was used to calculate the appropriate time for each distribution strategy to interfere with the vehicle movement. Simulation results under complex driving conditions showed that the proposed algorithm was verified to improve both the driving stability and fuel economy of the in-wheel vehicle.

Research conducted by Dizagah et al. [5] has provided an analytical relationship to calculate the range of torque required by a vehicle. It has been shown that adjusting the torque of the motors on one side of the vehicle is sufficient in most cases. They claim that their torque control strategy reduces energy consumption by up to 5% compared to the single-axle vehicles and the energy consumed on the corner is significantly reduced.

Koehler et al. [6] have implemented an optimization methods to find the yaw rate and slip angle, which minimizes energy consumption when EV is cornering. Then, by applying optimal control, they create the conditions for the vehicle to follow the desired values. They showed that energy consumption is reduced by about 10% on average acceleration at different conditions.

Phillips et al. [7] used the torque vectoring control of EVs with the aim of improving performance and reducing energy consumption. They showed that further significant energy consumption reductions can be achieved through the appropriate tuning of the reference understeer characteristics of the vehicle.

Sun et al. [8] investigated the effect of the torque-vectoring on traction energy conservation during cornering for a rear-wheel-independent-drive EV using an optimal torque vectoring control strategy based on genetic algorithm. Simulation results demonstrated that the torque-vectoring contribution can reach up to 1.7% in the tractive energy conservation of EVs.

Xu et al. [9] presented a novel braking torque distribution strategy for a EV with four in-wheel motors equipped with the regenerative braking system. Based on model predictive control (MPC) theory, the proposed torque distribution controller can maximize the regeneration efficiency by determining the hydraulic braking torque and motor braking torque. The simulations and the real-time test demonstrated the effectiveness of the optimal control strategy presented.

Hu et al. [10] proposed a stability-guaranteed and energy-conserving torque distribution strategy for the EVs according to the driver’s dynamic demand and actuator constraints based on MPC theory. The motor efficiency map is used in the objective function to reduce energy consumption while improving and balancing motor efficiency. The proposed torque distribution strategy showed an increment of energy saving under double lane change and straight acceleration maneuvers respectively, while the power loss does not exceed 8%.

In reference [11], an optimal torque vectoring control strategy based on a two-level distribution formula was proposed to reduce energy consumption while ensuring handling stability. By considering motor efficiency, the vehicle total torque is optimally distributed to the front and rear axles based on MPC. Then, based on the front/rear axle distribution ratio, the left/right torque vectoring is revised to produce a suitable additional yaw moment to improve the handling stability. The simulation and hardware-in-the-loop experimental results demonstrate that the proposed control strategy can reduce energy consumption while ensuring vehicle stability.

Wang et al. [12], designed an energy management strategy for four-wheel independent-drive electric vehicle (4WIDEV) based on multi-objective online optimization. The weighted yaw rate tracking error and electric drive system efficiency, tire slip losses and wheel torque ripple are included in the torque distribution strategy. The simulation results showed that the proposed four-wheel torque distribution strategy based on the multi-objective online optimization is more effective than average distribution strategy and offline optimization strategy.

The research paper [13], presents a proposed torque vectoring architecture intended to control the four electrical machines of a four-wheel-drive (4WD) formula-type competition vehicle. The architecture includes a newly developed yaw-rate controller, as well as an innovative optimal torque distribution algorithm. The design of both controllers utilizes an extended bicycle model that has been validated using experimental data. The simulation results demonstrate that the proposed control scheme is effective in enhancing energy efficiency, cornering speed, and stability, even in high-demanding working conditions.

Zhang et al. [14], proposed a hierarchical chassis control strategy for 4WIDEV that enhances vehicle economy and safety. The upper-level of the control strategy involves a vehicle dynamics model based on multiple agents and a distributed model predictive control (DMPC) method to track the center-of-mass torque of the demanded velocity trajectory and stability parameters. The bottom-level involves a multi-objective torque distribution strategy that weighs safety, dynamics, and economy based on multi-agent theory. This strategy comprehensively considers motor efficiency and tire energy loss. The proposed method was verified using a hardware-in-the-loop (HIL) simulation platform, and the results show that it is effective in tracking the desired trajectory and enhancing vehicle stability under various conditions.

In the research paper [15], an integrated torque distribution strategy was proposed that simultaneously considers vehicle safety and dynamic power allocation. In the upper layer, the integrated yaw stability and active front steering controller are developed to maintain vehicle stability. In the lower energy distribution layer, the motor efficiency and dynamic tire-slip power are simultaneously optimized to maintain EV energy conservation. The results demonstrate that the energy consumption of the powertrain is reduced by 13.4% and 14.2% under the steering and straight driving conditions, respectively.

Sun et al. [16] suggested a direct yaw moment control (DYC) for energy-efficiency and a DYC for stability of EVs. A switching principle for alternating between the two DYCs was designed based on the yaw rate and slip angle for evaluating the criticality of the vehicle's working state. During non-safety-critical cornering maneuvers, it is shown that DYC for energy efficiency can save considerable percentage of energy compared to both equal torque driving and the DYC for stability. During cornering maneuvers containing both non-safety-critical parts and safety-critical parts, the simulation results showed that the combination of two DYCs can give 12% to 18% energy savings compared to the DYC for stability only for the vehicle and maneuvers studied.

The authors of a research paper, Deng et al. [17], have proposed a novel torque vectoring control (TVC) method for electric vehicles with four in-wheel motors. This method combines safety and energy-saving performance using deep reinforcement learning (RL). The proposed control structure comprises two layers: an active safety control layer and a torque allocation layer based on RL. The paper includes numerical experiments to test the effectiveness of the proposed TVC method under different driving conditions. The results of the study show that the

[DOI: 10.22068/ase.2026.725]

proposed TVC method outperforms existing control methods in enhancing vehicle safety and energy efficiency while also reducing driver workload.

In reference [18], MPC methods for energy-efficient torque vectoring of four in-wheel motor electric vehicles, while ensuring stability are proposed. The methods use adaptive weighting factors based on exponential functions that vary with lateral motion and steering input. The predictive controller can be represented as either a Linear Parameter-Varying MPC (LPV-MPC) or Nonlinear MPC (NMPC), depending on the optimal control problem formulation. LPV-MPC decouples longitudinal and lateral motions, while NMPC exploits the coupled dynamics of the two-track model. The methods are compared and demonstrated in three driving scenarios using CarMaker simulation software, resulting in fuel efficiency improvements of over 2-3% on average with guaranteed yaw stability, compared to the built-in IPG driver in CarMaker.

In this paper, a sliding mode controller (SMC) is used to calculate the required total longitudinal force and yaw moment for an EV with four independent in-wheel motors to track the desired yaw rate and longitudinal velocity for improving the vehicle stability during the severe maneuver. Then, an optimal control allocation scheme is presented to provide optimally distributed torques of four in-wheel motors which can minimize the energy consumption and produce the longitudinal force and yaw moment calculated by the upper layer.

The remainder of this paper is organized as follows. Section 2 describes the vehicle model and electric motors. Section 3 details the design of the sliding mode controller and the optimal torque allocation scheme. Section 4 presents simulation results and discusses the performance of the proposed strategy. Finally, Section 5 concludes the paper and outlines future research directions.

2. Vehicle Modeling

Dynamic control of a vehicle requires mathematical modelling of its dynamic behavior. For this purpose, vehicle modelling is essential to simulate the dynamic behavior of the vehicle. Extensive research has been done on the dynamics of automotive modelling to achieve the parameters and variables that play a crucial role in controlling vehicle movement.

CarSim is the standard and convenient vehicle dynamics simulation software, and its computing power is more than three to six times faster than the actual situation. It can be used to realize the simulation analysis of vehicle response to the driver, road surface, and aerodynamic input. It can be used to achieve a simulation analysis of important indexes in vehicle handling stability, ride comfort, dynamic property, braking performance, and economy. CarSim software can define the simulation environment and simulation process according to the needs of developers. It can set the simulation parameters and characteristic files of vehicle control systems by itself. For simulating vehicle dynamic behavior in this study, a model of a four-in-wheel motor electric vehicle (as depicted in Figure 1) is developed in CarSim. The existing vehicle dynamics simulation models in CarSim software are designed for traditional internal combustion engine vehicles. The distributed drive EV model that we need to build is driven directly by in-wheel motors, which means that the original default engine, gearbox, differential, and other transmission systems in the CarSim model need to be deleted, as shown in Figure 1.

According to the vehicle parameters in Table 2, the dynamic model of the whole distributed drive EV is built. At the same time, the drive torque output model of an in-wheel motor is built to replace the original transmission system and realize the actual distributed drive EV modelling.

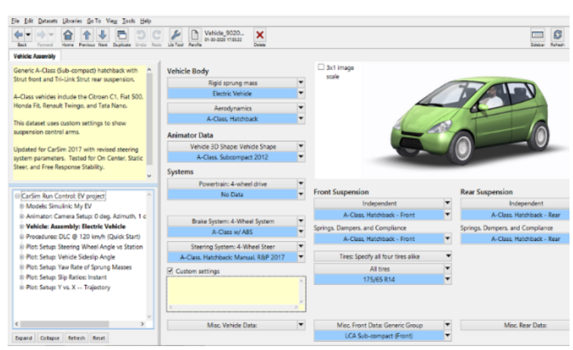

Figure 1: EV modeling in CarSim.

[DOI: 10.22068/ase.2026.725]

3.1. Electric motors

Permanent magnet synchronous motors (PMSM) have gained attention for in-wheel applications. The drive motors located at the empty space of the wheel are considered as a part of the un-sprung mass. Most electric motors on the market are too heavy to be installed in drive wheels. For an electric motor to be applicable in an EV with in-wheel motors, the low mass and high torque to mass ratio are two key factors [19]. Because the rotor in PMSM is a permanent magnet, the copper loss and magnetizing current present in the rotor of conventional DC motors are removed. Other than that, direct control of motor torque is easily accessible, which has brought great benefits to the in-wheel EVs. Because the motor drives dynamic response much faster than wheel dynamics, the electric motor and its controller can be simply modelled as a first-order delay system as the following transfer function:

$$G(s)=\frac{T_m}{T}=\frac{1}{(L_s/R_s)s+1} \tag{1}$$

Where R_s, L_s are the resistance and inductance of motor winding, respectively. $T(t)$ and $T_m(t)$ are the command torque obtained from torque distribution controller and the actual torque motor applied to the wheel, respectively.

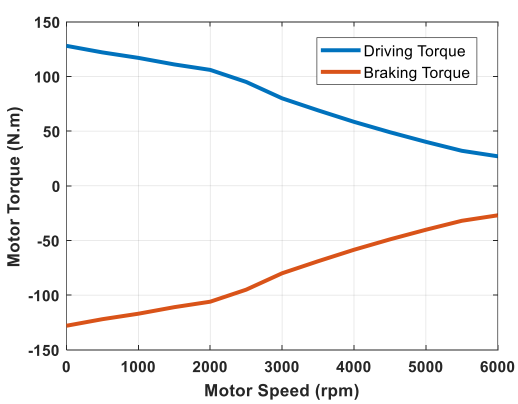

Figure 2: Driving torque and regenerative torque characteristics of in-wheel motor.

The PMSM used in this research is selected with the maximum speed of 6000 rpm, with a peak torque of 128 Nm, and the maximum power of 25 kW to meet the vehicle performance. As shown in Figure 3, the driving/braking torque limitation for each in-wheel motor is function of motor speed. Due to high-speed of selected electric motor, a speed reduction is used with reduction ratio of 2.

3. Controller Design

To improve the vehicle handling and stability, a multi-layered control system has been developed which consists of two layers, as illustrated in Figure 3. High-level is responsible to generate the total longitudinal force and yaw moment for every input command from the driver as well as yaw rate and longitudinal velocity signals from the vehicle. The control inputs generated from high-level controller are sent to low-level controller to be applied to the vehicle, which includes a torque allocation algorithm. This algorithm, based on the energy consumption of the in-wheel motors, determines the optimal torque applied by each of the motors so that the longitudinal force and yaw moment obtained from the high-level controller are produced in the vehicle.

3.2. Desired values generation

As the upper-level controller should minimize the difference between the vehicle response during maneuvers and the desired response, one of the most essential parts of the controller design is determining the desired response for the vehicle during the maneuver. Therefore, the two-degree-freedom model has been used to determine the desired values of yaw rate and longitudinal velocity of the vehicle. So a reference bicycle model is used as follows [20]:

$$u_d = u_0 + \int_0^t a_{xd}(\tau)\,d\tau \tag{2}$$

$$r_d = \frac{u\,\delta_f}{l+K_g u^2} \tag{3}$$

Where u_d and r_d are desired longitudinal velocity and yaw rate, respectively. K_g is the understeer gradient is determined by coefficients of the tire cornering stiffness at different vertical loads and road conditions, and δ_f is the front wheel angle. u_0 is initial longitudinal velocity and

[DOI: 10.22068/ase.2026.725]

a_{xd} represents the longitudinal acceleration based on the driver's input.

3.3. Upper-level controller design

Since the EV is a non-linear system operating under uncertain conditions such as changing the vehicle parameters and road conditions, the SMC technique is used for designing the high-level controller. To control the longitudinal and lateral vehicle dynamics, the longitudinal velocity and yaw rate of vehicle must be controlled in order that the actual values of these variables follow the desired values described in previous section. In order to design the SMC, the simplified equations for longitudinal and yaw motions of vehicle are used as follows:

$$\begin{cases} \dot{u} = \dfrac{1}{m}(F_{xd} - 0.5C_D A_f \rho_a u^2) \\ \dot{r} = \dfrac{1}{I_z} M_{zd} \end{cases} \tag{4}$$

The sliding mode surfaces are designed in the longitudinal motion and the yaw motion of the vehicle, respectively, to follow the desired vehicle status mentioned above, which are defined as:

$$\begin{cases} S_1 = u - u_d + \lambda_1 \int (u - u_d)\, dt \\ S_2 = r - r_d + \lambda_2 \int (r - r_d)\, dt \end{cases} \tag{5}$$

The sliding mode control objective is to reach and remain in the sliding surface such that $\dot{S} = 0$ based on equation (5). So, the control laws u_1 and u_2 are directly derived from the sliding surfaces [21]. To have better control performance regarding the chattering phenomenon, the saturation function instead of the sign function is adopted in the process of control design, which is given by:

$$\begin{cases} \dot{s}_n = -k_n sat(\dfrac{s_n}{\phi_n}) \qquad \forall n \in \{1,2\} \\ sat(\dfrac{s_n}{\phi_n}) = \begin{cases} \dfrac{s_n}{\phi_n} & if\, |s_n| < \phi_n \\ \operatorname{sgn}(\dfrac{s_n}{\phi_n}) & if\, |s_n| \ge \phi_n \end{cases} \end{cases} \tag{6}$$

The coefficient k_n is a positive constant determining the approaching rate of the system state on the sliding surface, the coefficient ϕ_n is used to smooth the control discontinuity in the law of sliding mode and also determines the tracking errors. The larger the value, the less the chattering, but the convergence rate of the system is slower. According to the principle of SMC, the control laws are ultimately given by:

$$\begin{cases} u_1 = F_{xd} = m\,(a_{xd} - k_1 sat(\dfrac{s_1}{\phi_1}) - \lambda_1 (u - u_d)) \\ \qquad + \dfrac{1}{2} C_D A_f \rho_a u^2 \\ u_2 = M_{zd} = I_z[(\dfrac{a_{xd}(l - K_g u^2)\delta_f}{(l + K_g u^2)^2}) - k_2 sat(\dfrac{s_2}{\phi_2}) \\ \qquad - \lambda_2 (r - r_d)] \end{cases} \tag{7}$$

where F_{xd} and M_{zd} are obtained to pursue the best tracking performance; meanwhile, they act as inputs of the low-level controller, which generates the desired driving/braking torque commands for the four electric motor controllers. The control parameters of the sliding mode controller are listed in Table 1, through a lot of simulation results.

Table 1 Parameters of the sliding mode controller.

Coefficient	γ_1	γ_2	ϕ_1	ϕ_2	λ_1	λ_2
Value	2	2.3	0.1	0.1	0.5	0.5

3.4. Lower-level controller design

Because the control inputs obtained from the upper-level controllers are corrective yaw moment and total longitudinal force, to apply these control inputs to the vehicle, the lower-level controllers must be used. The task of the lower-level controller, which is an optimal control allocation, is to properly distribute the wheel torques based on the torque distribution algorithm. The control torques obtained from the lower-level controller, as reference torques, are considered separately for the electric motor controllers of each wheel. Then, the output of these electric motor controllers is the torque applied to the vehicle wheels. The torques of the in-wheel motors produce the required longitudinal forces in the wheels, which ultimately achieve the desired total longitudinal force and yaw moment obtained from the upper-level controller.

The control allocation method is usually used when the number of system actuators exceeds the number of states intended to control. As the number of actuators of vehicles (four in-wheel motors) is greater than the number of states intended to control (longitudinal velocity and yaw rate of the vehicle), the EV with four independent in-wheel motors is an over-actuated system. So, the task of the control allocation algorithm is to distribute command torques to the controllers of the four in-wheel motors. In the method presented in this paper, the torque allocation algorithm, based on the energy consumption of the electric motors, determines the optimal torque applied by each of the electric motors, so that total longitudinal force and yaw moment obtained from the upper level are created in the vehicle. According to Figure 4, and assuming the small steering angle, the total longitudinal force and the yaw moment can be expressed as the following relations:

$$F_{xd} = F_{xfl} + F_{xfr} + F_{xrl} + F_{xrr} \tag{8}$$

$$M_{zd} = (-F_{xfl} + F_{xfr})\frac{t_f}{2} + (-F_{xrl} + F_{xrr})\frac{t_r}{2} \tag{9}$$

The above equations are used as two equality constraints in energy consummation optimization described in following section.

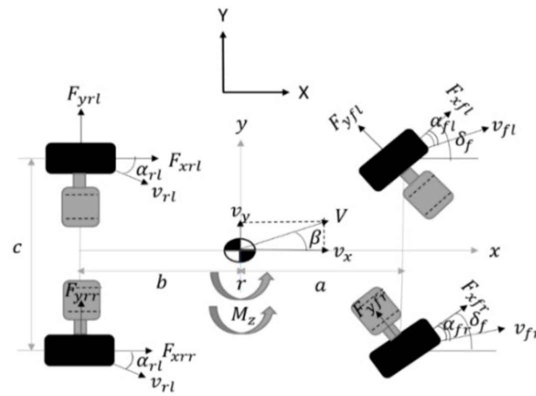

Figure 4. Schematic of four-wheel vehicle model

3.4.1. Torque distribution algorithm based on energy consumption optimization

In this section, according to the desired longitudinal force F_{xd} and the yaw moment M_{zd} at each time step calculated by the upper-level controller, the proposed energy-efficient method minimizes the electric motor power consumption subject to the two equality constraints (8) and (9). In addition, the driving torque should be allocated adequately such that each of the driving or braking force produced in each wheel do not exceed maximum motor torque as well as the maximum value of road adhesion force which is equal to tire vertical force multiply by tire-road friction coefficient. When the vehicle works in an acceleration mode, the vertical load will transfer to the rear wheels from the front wheels, and vice versa during the deceleration process. Therefore, under different conditions, the maximum of road adhesion force is changed by load shift, which can be considered a constraint in the optimization model [22]. Therefore**,** the allocation problem based on energy efficiency is transformed into a nonlinear optimization problem, the energy optimization function and constraints are described mathematically in the following section, assuming that the efficiency map of four electric motors is the same with identical power consumption characteristics.

The energy efficiency optimization problem of distributed drive EVs can be converted into minimal instantaneous power consumption, which can be represented as a function of the

[DOI: 10.22068/ase.2026.725]

four-wheel torques. The power of motors is directly related to their torque. The motor torque on the wheel as the optimization variable is expressed as $T=[T_{m-fl} \quad T_{m-fr} \quad T_{m-rl} \quad T_{m-rr}]$, which represents the motor torques on the front left wheel, front right wheel, rear left wheel, and rear right wheel respectively. Because the in-wheel motor can perform in motor or generator mode, they can generate both driving and braking torque. According to that, the electric power consumption of in-wheel motors at each wheel are given by:

$$P_c(T_m)=\begin{cases}\dfrac{T_m\,\omega}{\eta_m(\omega,T_m)} & if \quad T_m>0\\ T_m\,\omega\,\eta_g(\omega,T_m) & if \quad T_m<0\end{cases} \tag{10}$$

Where η_m is the efficiency in the motor mode and η_g is the efficiency in the generator mode.

The power consumption of all four electric motors is expressed as follows:

$$P_{c\_total}(T_{m-ij})=\sum_{\substack{i=f,r\\ j=l,r}} P_c(T_{m-ij}) \tag{11}$$

Electric motor efficiency contour of the selected PMSM is shown in Figure 5.

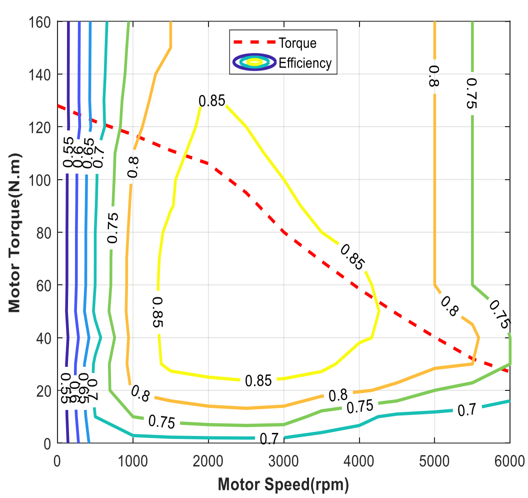

Figure 5. Electric motor efficiency contour

Since only the efficiency in the motor mode can be obtained from this contour, one can calculate the efficiency in generator mode from efficiency in the motor mode by assuming equal power loss in motor and generator mode:

$$P_{loss,m}=P_{loss,g}\Rightarrow T_m\omega(\frac{1}{\eta_m}-1)=T_m\omega(1-\eta_g)$$
$$\Rightarrow \eta_g=2-\frac{1}{\eta_m} \tag{12}$$

In general, the cost function can be designed as follows:

$$J=\min P_{c-total}(T_{m-ij})=\sum_{i=fl,fr,rl,rr} P_{ci}(T_{mi}) \tag{13}$$

The constraints of the energy efficiency optimization problem consist of equality and inequality constraints. The two equality constraints meet the demands of the upper-level controller, including the desired longitudinal force F_{xd} and the yaw moment M_{zd} .The equation (8) and (9) are rewritten according to motor torque and speed reduction ratio as follows:

$$F_{xd}=\frac{n_g}{r_w}(T_{m-fl}+T_{m-fr}+T_{m-rl}+T_{m-rr}) \tag{14}$$

$$M_{zd}=\frac{n_g}{r_w}[\frac{t_f}{2}(T_{m-fr}-T_{m-fl})+\frac{t_r}{2}(T_{m-rr}-T_{m-rl})] \tag{15}$$

Where r_w is the radius of the wheels assuming it is a constant when driving and n_g is the electric speed reduction ratio, t_f and t_r are front and rear vehicle track, respectively. As mentioned before, inequality constraints, limitations of the motor capacity and road adhesion force are considered. The limitations of the motor capacity are expressed below:

$$-T_{m\_ij\_\max}(\omega)\le T_{m\_ij}\le T_{m\_ij\_\max}(\omega) \tag{16}$$

Where $T_{m\_\max}$ is the maximum motor torque which is function of motor speed according to Figure 4. The vertical force of each wheel can be calculated as following equations:

[DOI: 10.22068/ase.2026.725]

$$
\begin{aligned}
F_{z-fl} &= \frac{mgl_r}{2l} - \frac{ma_x h_g}{2l} - \frac{mb}{l}\frac{a_y h_g}{t_f} \\
F_{z-fr} &= \frac{mgl_r}{2l} - \frac{ma_x h_g}{2l} + \frac{mb}{l}\frac{a_y h_g}{t_f} \\
F_{z-rl} &= \frac{mgl_f}{2l} + \frac{ma_x h_g}{2l} - \frac{ma}{l}\frac{a_y h_g}{t_r} \\
F_{z-rr} &= \frac{mgl_f}{2l} + \frac{ma_x h_g}{2l} - \frac{ma}{l}\frac{a_y h_g}{t_r}
\end{aligned} \tag{17}
$$

where F_{z-ij} is the vertical tire force, m is the vehicle wheelbase, m is the total mass of the vehicle, a_x and a_y are the vehicle longitudinal and lateral acceleration, h_g is the vehicle CG height, l_f and l_r are the distances from vehicle CG to the front and rear axles. According to the cost function and the constraints, the energy-efficient optimization scheme is described as:

$$
\begin{aligned}
&\min \quad J = \sum_{i=fr,fl,rl,rr} p_{ci} \\
&F_{xd} = \frac{n_g}{r_w}(T_{m-fl} + T_{m-fr} + T_{m-rl} + T_{m-rr}) \\
&M_{zd} = \frac{n_g}{r_w}[\frac{t_f}{2}(T_{m-fr} - T_{m-fl}) + \frac{t_r}{2}(T_{m-rr} - T_{m-rl})] \\
&T_{m\_i\_\min}(\omega_{mi}) \le T_{m\_i}(\omega_{mi}) \le T_{m\_i\_\max}(\omega_{mi}) \\
&n_g |T_{m-i}| \le \mu F_{z-i} r_w
\end{aligned} \tag{18}
$$

Through the above analysis, the optimization allocation scheme is formulated as a nonlinear programming problem, which is expressed in equation (18), which is solved using the MATLAB function *fmincon*, with the Sequential Quadratic Programming (SQP) method as the solution algorithm [23]. For comparing the performance of the proposed control allocation algorithm, another toque distribution algorithm based on the dynamic tire vertical load is presented as following section.

3.4.2. Torque distribution algorithm based on dynamic load distribution

Due to dynamic weight transfer based on longitudinal and lateral accelerations, vertical tire forces are not equal when driving and cornering. Furthermore, the maximum longitudinal force that can be generated in a tire is directly pertinent to tire-road friction as well as its vertical force. Therefore, the impact of vertical forces in the control allocation algorithm should be taken into consideration because the more a tire can generate longitudinal force in terms of its vertical force, the more torque can be applied to that tire and vice versa. In this case, the individual longitudinal force of each tire can be used effectively. In this approach, the corrective yaw moment and total longitudinal force obtained from the upper-level controller are distributed in terms of vertical force of each tire. So, we have:

$$\frac{F_{x,fl}}{F_{x,rl}} = \frac{F_{zfl}}{F_{zrl}} = \rho_L \tag{19}$$

$$\frac{F_{x,fr}}{F_{x,rr}} = \frac{F_{zfr}}{F_{zrr}} = \rho_R \tag{20}$$

where ρ_R and ρ_L are the front to rear vertical tire force ratio of left and right side of vehicle respectively. The equations (14) and (15) and (19) and (20) can be rewritten as:

$$T_{m-fl} + T_{m-fr} + T_{m-rl} + T_{m-rr} = \frac{F_{xd} r_w}{n_g} \tag{21}$$

$$\frac{t_f}{2}T_{m-fr} - \frac{t_f}{2}T_{m-fl} + \frac{t_r}{2}T_{m-rr} - \frac{t_r}{2}T_{m-rl} = \frac{M_{zd} r_w}{n_g} \tag{22}$$

$$T_{m-fl} - \rho_L\, T_{m-rl} = 0 \tag{23}$$

$$T_{m-fr} - \rho_R\, T_{m-rr} = 0 \tag{24}$$

The equations (21) to (24) can be rewritten as following matrix form and solved for obtaining the command torque of four in-wheel electric motor controller:

$$
\begin{bmatrix}
1 & 1 & 1 & 1 \\
-\frac{t_f}{2} & \frac{t_f}{2} & -\frac{t_r}{2} & \frac{t_r}{2} \\
1 & -\rho_L & 0 & 0 \\
0 & 0 & 1 & -\rho_R
\end{bmatrix}
\begin{bmatrix}
T_{m-fl} \\ T_{m-fr} \\ T_{m-rl} \\ T_{m-rr}
\end{bmatrix}
=
\begin{bmatrix}
\frac{F_{xd} r_w}{n_g} \\ \frac{M_{zd} r_w}{n_g} \\ 0 \\ 0
\end{bmatrix} \tag{25}
$$

4. Simulation Results

To verify the effectiveness of the proposed control algorithm, two maneuvers, including J-turn and lane change, are investigated by MATLB/ Simulink and CarSim simulation in similar road conditions.

Table 2 Vehicle and electric motor parameters

Parameter (unit)	Value	Parameter (unit)	Value
$m(kg)$	850	$\rho_a(kg/m^3)$	1.206
$I_z(kgm^2)$	930	$A_f(m^2)$	1.6
$l_f\ (m)$	0.81	C_d	0.4
$l_r(m)$	0.99	$K_g(\frac{rad.s^2}{m})$	0.004
$l(m)$	1.8	$P_{\max}(kW)$	25
$h_g\ (m)$	0.51	$T_{\max}(Nm)$	128
$r_w(m)$	0.26	$L_s(H)$	0.003
$t_f(m)$	1.415	$R_s(\Omega)$	0.3
$t_r(m)$	1.375	n_g	2

The typical A-class sedan vehicle model is chosen from CarSim database. In the CarSim, a vehicle model was built by making use of its own sub models. The CarSim vehicle model has been validated with the experimental results of an actual vehicle. The specific part of vehicle data that is used in the CarSim simulations is given in Table 1.

4.1. J-turn maneuver on dry road

In this maneuver, the vehicle travels at a constant speed of 60 km/h on a dry road with the tire-road adhesion coefficient of 1. A J-turn is then initiated by a steering wheel angle input of 90°. Figure 6 shows the responses of controlled and uncontrolled vehicles for this type of input. As Figure 6(b) shows the sideslip angle of the uncontrolled vehicle has a large maximum value, which means the vehicle is in an undesired condition.

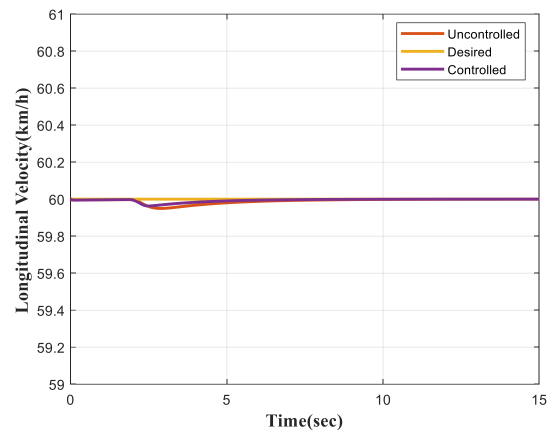

(a)

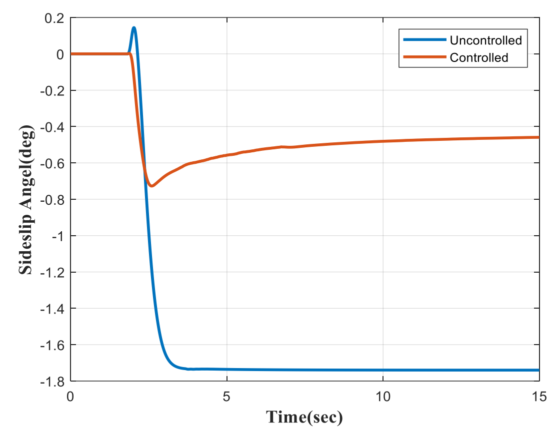

(b)

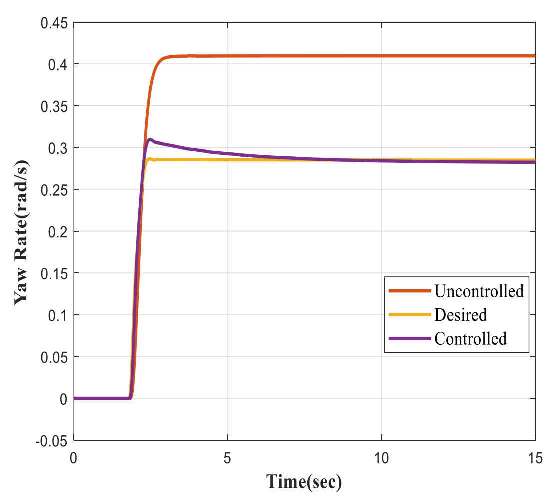

(c)

[DOI: 10.22068/ase.2026.725]

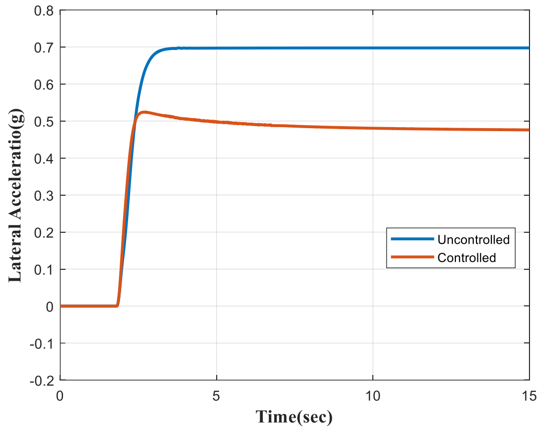

(d)

Figure 6. Vehicle simulation in J-turn maneuver on dry road; (a) vehicle longitudinal velocity (km/h), (b) sideslip angle (deg), (c) yaw rate (deg/s), (d) lateral acceleration (g).

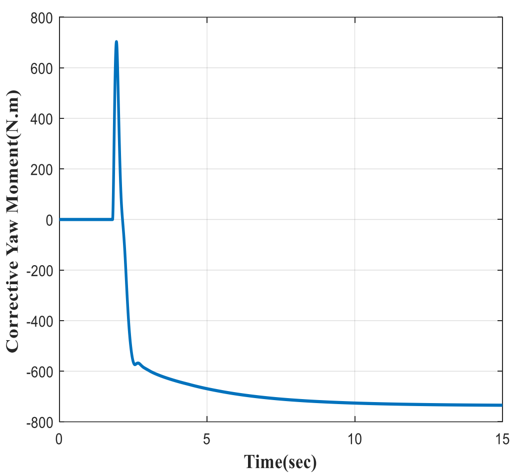

(a)

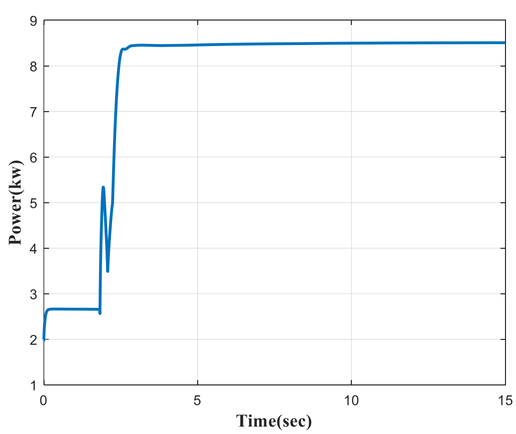

(b)

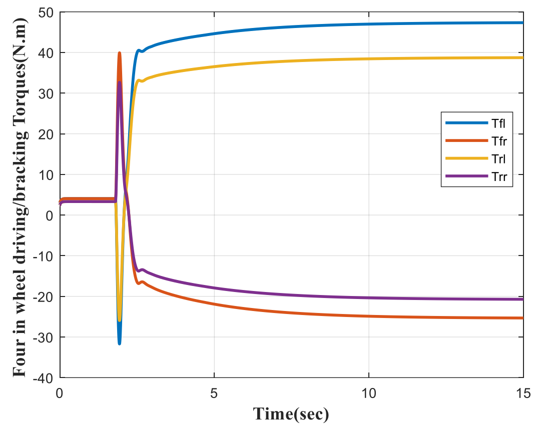

(c)

Figure 7. Vehicle simulation in J-turn maneuver on dry road; (a) corrective yaw moment (Nm), (b) motors power consumption (kW), (c) driving/braking torques of each wheel.

4.2. Lane change maneuver on slippery road

In this maneuver, the EV performs a lane change maneuver while accelerating on slippery road with friction coefficient of 0.5. The driver steering wheel angle applied by driver is shown in Figure 8(a). The longitudinal velocity, yaw rate, sideslip angle, lateral acceleration of the controlled and uncontrolled vehicle are shown in Figure 8(b) to 8(e). As shown in Figure 8(b), the longitudinal velocity of controlled vehicle is increased with acceleration of 0.1g while the uncontrolled vehicle longitudinal velocity is decreased because the sideslip angle of uncontrolled EV increases rapidly during lane change as shown in Figure 8(c). It also demonstrates that the sideslip angle of the controlled vehicle is kept small and the vehicle perform lane change maneuver in a stable region. Figure 8(d) shows that the controller can trace the desired yaw rate during lane change maneuver while the uncontrolled vehicle cannot follow the desired yaw rate and slides in second section of maneuver. Figure 8(e) also shows that the lateral acceleration of the controlled vehicle is like the driver steering wheel demand while the uncontrolled vehicle lateral acceleration become saturated due to low road friction coefficient. The motor torque applied to each wheel and motors power consumption are shown in Figure 9.

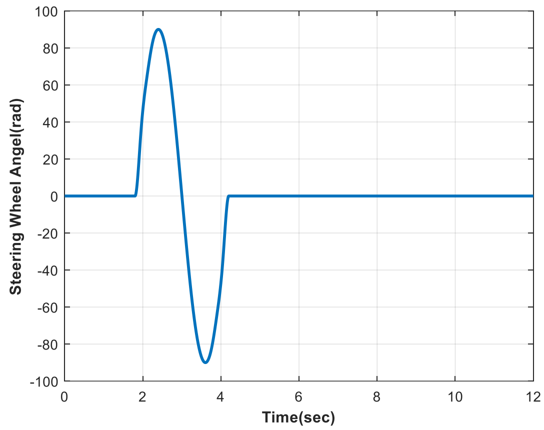

(a)

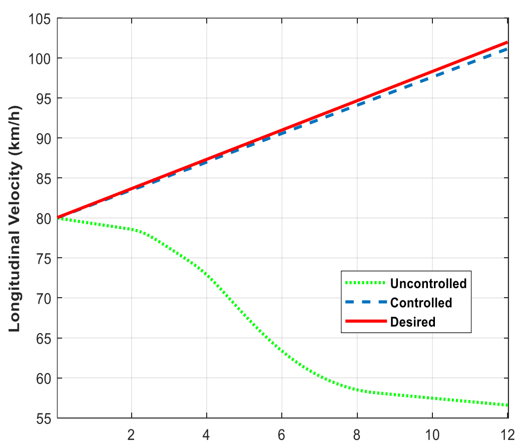

(b)

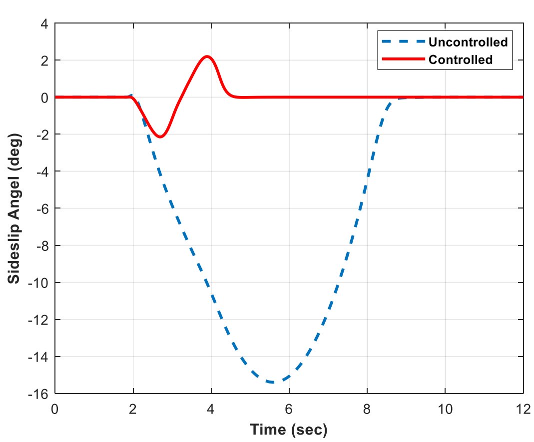

(c)

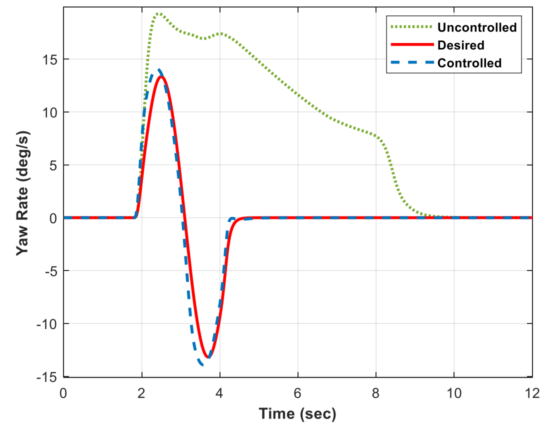

(d)

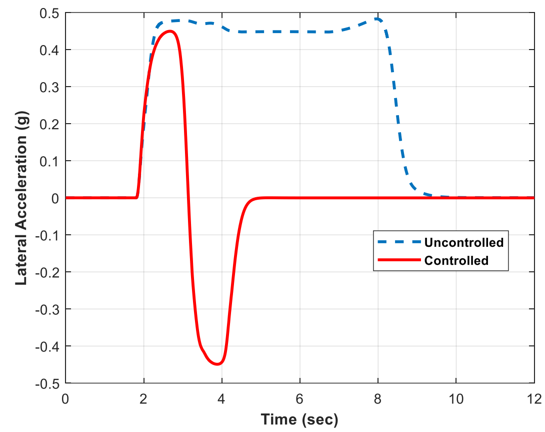

(e)

Figure 8. Simulation results in lane change on slippery road; (a) steering wheel angle (deg), (b) vehicle longitudinal velocity (km/h), (c) yaw rate (deg/s), (d) sideslip angle (deg), (e) lateral acceleration (g).

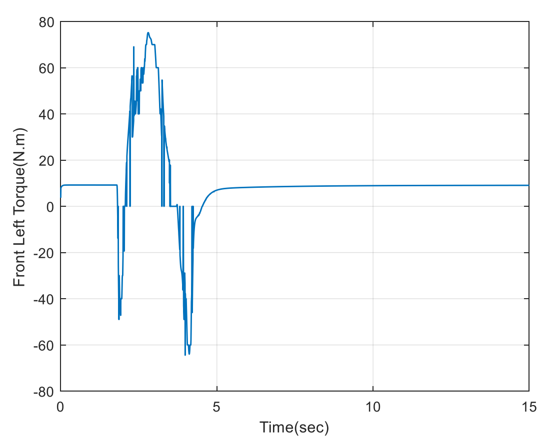

(a)

[DOI: 10.22068/ase.2026.725]

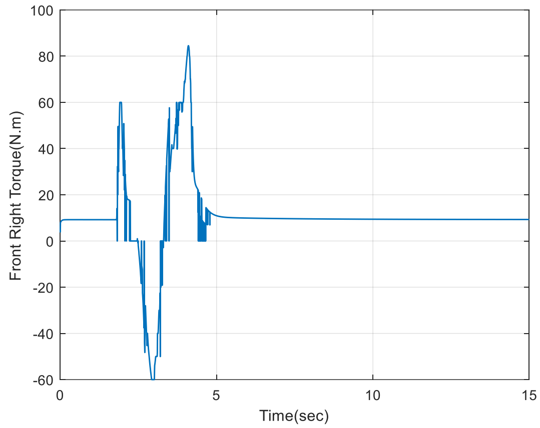

(b)

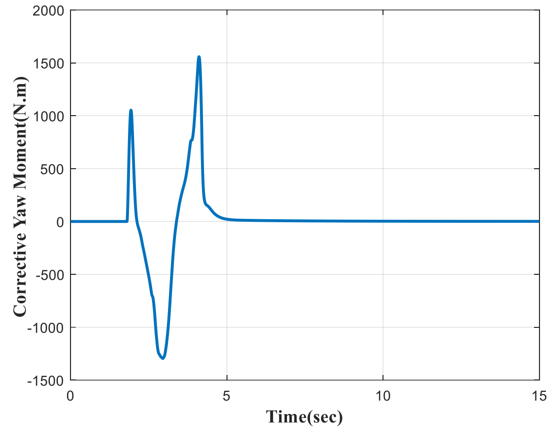

(e)

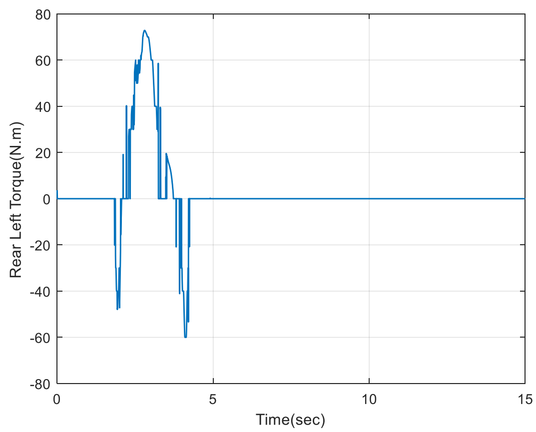

(c)

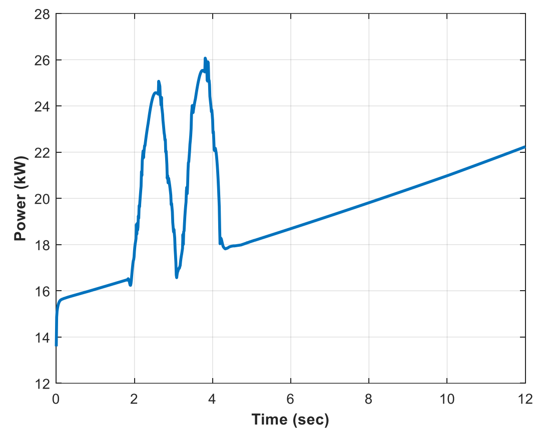

(f)

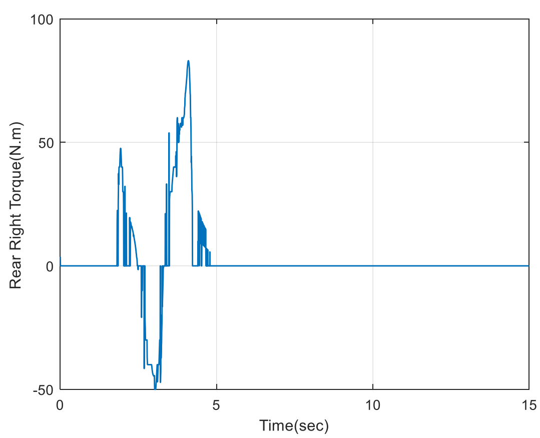

(d)

Figure 9. Vehicle simulation in lane change maneuver on slippery road; (a) front left motor torque (Nm), (b) front right motor torque (Nm), (c) rear left motor torque (Nm), (d) rear right motor torque (Nm), (e) corrective yaw moment (Nm), (f) motors power consumption (kW).

The controller performance to track the desired longitudinal velocity and yaw rate in two simulations are shown in Table 3. As shown in Table 3, the root mean square (RMS) errors of tracking the desired longitudinal velocity and yaw rate are small.

Table 1 Tracking error of controller

RMS error	Velocity tracking error	Yaw rate tracking error
J-turn maneuver	1.5 deg/s	0.5 km/h
Lane-change maneuver	1.258 deg/s	1.5 km/h

The power consumption of electric motors during lane change maneuver with constant longitudinal velocity of 70 kph with two torque distribution algorithms is compared in Figure 10. Figure 10 showed about ten percent improvement in energy saving for the proposed torque distribution compared to conventional dynamic load algorithm.

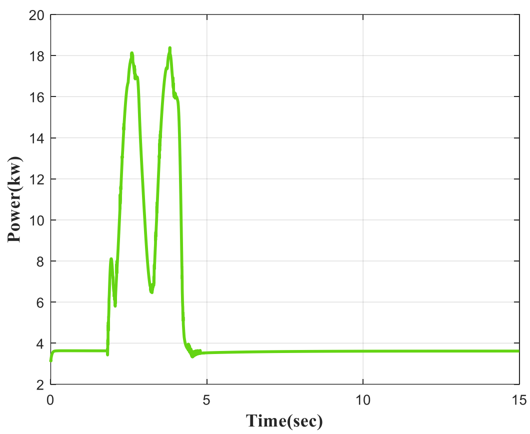

(a)

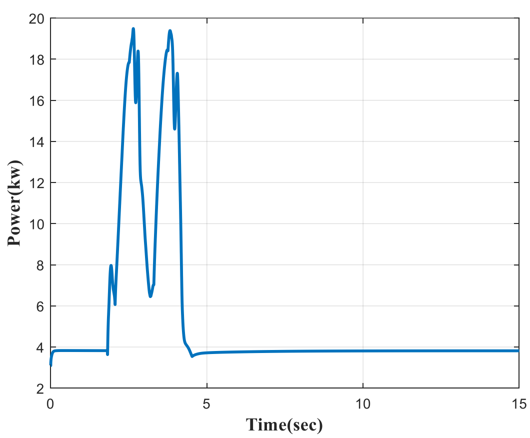

(b)

Figure 10. Vehicle simulation in lane change maneuver on slippery road; (a) motors power consumption in torque distribution algorithm based on energy consumption optimization, (b) motors power consumption of the torque distribution algorithm is based on dynamic load transfer.

5. Conclusions

An energy efficiency optimization allocation method to reduce power consumption, from the electric motor drives of a distributed EVs with equal drivetrains on the front and rear axles, has been proposed during various maneuvers at the low-level controller. Furthermore, at the high-level controller, the desired torque and yaw moment are figured out based on sliding mode control. Moreover, energy regeneration has accounted for a large proportion of the total energy consumption, which should be utilized sufficiently. Through the analysis of simulation results under different conditions, the conclusion that theoretically, under all normal driving or braking conditions, the total torque should be distributed evenly to four motors to minimize motor power consumption is drawn. Future control allocation algorithms should take different sources of dissipation into account, such as tire slip, which is an important factor at significant acceleration levels.

List of symbols

a_x	Longitudinal acceleration
a_y	Lateral acceleration
F_{xd}	Desired longitudinal force
F_x	Longitudinal force
F_y	Lateral force
l_f	Distance from C.G. to front axle
l_r	Distance from C.G. to rear axle
M_{zd}	Corrective yaw moment
n_g	Reduction gear ratio
g	Gravitational acceleration
u	Longitudinal velocity
r_w	Tire rolling radius
r	Yaw rate
m	Vehicle mass
A_f	Front area
t	Vehicle track
δ_f	Steering angle
μ	Friction coefficient
ω	Wheel angular velocity

References

[1] D. Wang, C. Guan, J. Wang, H. Wang, Z. Zhang, D. Guo, and F. Yang, Review of Energy-Saving Technologies for Electric Vehicles, from the Perspective of Driving Energy Management, Sustainability, Vol. 15, No. 9, (2023), pp. 7617.

[2] A. Khajepour, M. S. Fallah, and A. Goodarzi, Electric and Hybrid Vehicles: Technologies, Modeling and Control-A Mechatronic Approach. John Wiley & Sons, NY (2014).

[3] B. Mashadi and M. Majidi, Integrated AFS/DYC sliding mode controller for a hybrid electric vehicle, International Journal of Vehicle Design, Vol. 56, No. 1-4, (2011), pp. 246–269.

[4] J. Park, H. Jeong, I. G. Jang, and S.-H. Hwang, Torque distribution algorithm for an independently driven electric vehicle using a fuzzy control method, Energies, Vol. 8, No. 8, (2015), pp. 8537–8561.

[5] A. M. Dizqah, B. Lenzo, A. Sorniotti, P. Gruber, S. Fallah, and J. De Smet, A fast and parametric torque distribution strategy for four-wheel-drive energy-efficient electric vehicles, IEEE Transactions on Industrial Electronics, Vol. 63, No. 7, (2016), pp. 4367–4376.

[6] S. Koehler, A. Viehl, O. Bringmann, and W. Rosenstiel, Energy-efficiency optimization of torque vectoring control for battery electric vehicles, IEEE Intelligent Transportation Systems Magazine, Vol. 9, No. 3, (2017), pp. 59–74.

[7] G. De Filippis, B. Lenzo, A. Sorniotti, P. Gruber, and W. De Nijs, Energy-efficient torque-vectoring control of electric vehicles with multiple drivetrains, IEEE Transactions on Vehicular Technology, Vol. 67, No. 6, (2018), pp. 4702–4715.

[8] W. Sun, J. Wang, Q. Wang, F. Assadian, and B. Fu, Simulation investigation of tractive energy conservation for a cornering rear-wheel-independent-drive electric vehicle through torque vectoring, Science China Technological Sciences, Vol. 61, No. 2, (2018), pp. 257–272.

[9] W. Xu, H. Chen, H. Zhao, and B. Ren, Torque optimization control for electric vehicles with four in-wheel motors equipped with regenerative braking system, Mechatronics, Vol. 57, (2019), pp. 95–108.

[10] X. Hu, P. Wang, Y. Hu, and H. Chen, A stability-guaranteed and energy-conserving torque distribution strategy for electric vehicles under extreme conditions, Applied Energy, Vol. 259, (2020), pp. 114162.

[11] X. Hu, H. Chen, Z. Li, and P. Wang, An energy-saving torque vectoring control strategy for electric vehicles considering handling stability under extreme conditions, IEEE Transactions on Vehicular Technology, Vol. 69, No. 10, (2020), pp. 10787–10796.

[12] J. Wang, S. Gao, K. Wang, Y. Wang, and Q. Wang, Wheel torque distribution optimization of four-wheel independent-drive electric vehicle for energy efficient driving, Control Engineering Practice, Vol. 110, (2021), pp. 104779.

[13] E. Morera-Torres, C. Ocampo-Martinez, and F. D. Bianchi, Experimental modelling and optimal torque vectoring control for 4WD vehicles, IEEE Transactions on Vehicular Technology, Vol. 71, No. 5, (2022), pp. 4922–4932.

[14] Z. Zhang, H. Ding, K. Guo, and N. Zhang, A Hierarchical Control Strategy for FWID-EVs Based on Multi-Agent with Consideration of Safety and Economy, Energies, Vol. 15, No. 23, (2022), pp. 9112.

[15] H. Wei, Q. Ai, W. Zhao, and Y. Zhang, Modelling and experimental validation of an EV torque distribution strategy towards active safety and energy efficiency, Energy, Vol. 239, (2022), pp. 121953.

[16] P. Sun, A. S. Trigell, L. Drugge, and J. Jerrelind, Energy efficiency and stability of electric vehicles utilising direct yaw moment control, Vehicle system dynamics, Vol. 60, No. 3, (2022), pp. 930–950.

[17] H. Deng, Y. Zhao, F. Lin, and Q. Wang, Deep Reinforcement Learning-Based Torque Vectoring Control Considering Economy and Safety, Machines, Vol. 11, No. 4, (2023), pp. 459.

[18] S. H. Kim and K.-K. K. Kim, Model Predictive Control for Energy-efficient Yaw-stabilizing Torque Vectoring in Electric Vehicles with Four In-wheel Motors, IEEE Access, (2023).

[19] F. Tahami, R. Kazemi, and S. Farhanghi, A novel driver assist stability system for all-wheel-drive electric vehicles, IEEE Transactions on vehicular Technology, Vol. 52, No. 3, (2003), pp. 683–692.

[20] Z. Wang, Y. Wang, L. Zhang, and M. Liu, Vehicle stability enhancement through hierarchical control for a four-wheel-independently-actuated electric vehicle, Energies, Vol. 10, No. 7, (2017), pp. 947.

[21] P. Song, C.-f. Zong, and M. Tomizuka, A terminal sliding mode based torque distribution control for an individual-wheel-drive vehicle, Journal of Zhejiang University SCIENCE A, Vol. 15, No. 9, (2014), pp. 681–693.

[22] R. Wang, Y. Chen, D. Feng, X. Huang, and J. Wang, Development and performance characterization of an electric ground vehicle with independently actuated in-wheel motors, Journal of Power Sources, Vol. 196, No. 8, (2011), pp. 3962–3971.

[23] J. H. Plumlee, D. M. Bevly, and A. S. Hodel, Control of a ground vehicle using quadratic programming based control allocation techniques, in Proc. of the 2004 American control conference, Boston, MA, USA, 2004, Vol. 5: IEEE, pp. 4704–4709.

[DOI: 10.22068/ase.2026.725]